RadioGraphics

Benign versus Malignant Hepatic Nodules: MR Imaging Findings with Pathologic Correlation[1]

Shahid M. Hussain, MD, PhD • Pieter E. Zondervan, MD
Jan N. M. IJzermans, MD, PhD • Solko W. Schalm, MD, PhD
Rob A. de Man, MD, PhD • Gabriel P. Krestin, MD, PhD

According to the currently used nomenclature, there are only two types of hepatocellular nodular lesions: regenerative lesions and dysplastic or neoplastic lesions. Regenerative nodules include monoacinar regenerative nodules, multiacinar regenerative nodules, cirrhotic nodules, segmental or lobar hyperplasia, and focal nodular hyperplasia. Dysplastic or neoplastic nodules include hepatocellular adenoma, dysplastic foci, dysplastic nodules, and hepatocellular carcinoma (HCC). Many of these types of hepatic nodules play a role in the de novo and stepwise carcinogenesis of HCC, which comprises the following steps: regenerative nodule, low-grade dysplastic nodule, high-grade dysplastic nodule, small HCC, and large HCC. State-of-the-art magnetic resonance (MR) imaging facilitates detection and characterization in most cases of hepatic nodules. State-of-the-art MR imaging includes single-shot fast spin-echo imaging, in-phase and opposed-phase T1-weighted gradient-echo imaging, T2-weighted fast spin-echo imaging with fat saturation, and two-dimensional or three-dimensional dynamic multiphase contrast material–enhanced imaging.

Abbreviations: FNH = focal nodular hyperplasia, HCC = hepatocellular carcinoma, H-E = hematoxylin-eosin

Index terms: Liver, focal nodular hyperplasia, 761.3198 • Liver, MR, 761.121411, 761.121412, 761.12143 • Liver, nodules, 761.319, 761.32 • Liver neoplasms, diagnosis, 761.319, 761.32

RadioGraphics 2002; 22:1023–1039

[1]From the Departments of Radiology (S.M.H., G.P.K.), Pathology (P.E.Z.), Surgery (J.N.M.I.), and Hepatology (S.W.S., R.A.d.M.), Erasmus University Medical Center, Dr Molewaterplein 40, 3015 GD Rotterdam, the Netherlands. Recipient of a Certificate of Merit award for an education exhibit at the 2001 RSNA scientific assembly. Received February 6, 2002; revision requested March 26 and received April 30; accepted May 3. **Address correspondence to** S.M.H. (e-mail: *smhussain62@hotmail.com*).

See the commentary by Heiken following this article. See also the article by Kim et al (pp 1041–1051) in this issue.

Introduction

Various parenchymal liver diseases may lead to hepatitis, fibrosis, and eventually cirrhosis. Cirrhotic liver contains regenerative nodules and may also contain dysplastic nodules as well as hepatocellular carcinoma (HCC) (1). By understanding the transition from benign through dysplastic to malignant nodules, one can more easily make sense of the complex nodularity depicted in cirrhotic livers with multiple magnetic resonance (MR) imaging pulse sequences (2–4).

During the past 2 decades, MR imaging has emerged as an important imaging modality for assessing cirrhosis and its complications, such as hepatic nodules (1). For assessment of hepatic nodules, MR imaging is more useful than any other imaging modality currently available (1).

The state-of-the-art MR imaging technique at our institution includes single-shot fast spin-echo images with shorter and longer echo times, in-phase and opposed-phase T1-weighted gradient-echo images, T2-weighted fast spin-echo images with fat suppression, a timing-bolus sequence, and two-dimensional or three-dimensional thin-section dynamic multiphasic gadolinium-enhanced images. The single-shot images serve as (*a*) localizers and (*b*) sequences for characterizing lesions (solid vs nonsolid) on the basis of the echo time. The in-phase and opposed-phase images can be used to detect focal or diffuse abnormalities. The T2-weighted fast spin-echo sequence with fat suppression is a very sensitive sequence for focal liver lesions. The timing-bolus sequence allows more reliable imaging of the liver in the arterial phase, which is crucial for detection of hypervascular liver lesions, such as adenomas, focal nodular hyperplasia (FNH), and HCC. The multiphasic dynamic sequences show the enhancement patterns of liver lesions, which are very helpful in characterization of the lesions. In addition, MR imaging with tissue-specific contrast media can be advocated to answer certain questions that might remain after MR imaging with gadolinium contrast material (eg, if the results of the gadolinium-enhanced MR imaging study are not conclusive concerning the hepatocellular origin of the tumor).

This article describes and illustrates current concepts about hepatic nodules. Specific topics discussed are etiologic factors, currently used terminology, pathways of carcinogenesis, histopathologic features, and MR imaging features.

Etiologic Factors

Except for FNH, hepatic nodules usually develop in previously damaged livers. Damage to the liver can be caused by several factors (5,6):

1. Endemic: Aflatoxin, a product of the fungus *Aspergillus flavus*, which grows on improperly stored grain and nuts (including peanuts), is considered an important cause of HCC in Africa and Asia.

2. Metabolic and genetic disorders, including hemochromatosis (increased hepatocellular iron deposition), Wilson disease (increased hepatocellular copper deposition), and α_1-antitrypsin deficiency, can lead to cirrhosis, hepatic nodules, and HCC.

3. Dietary: Obesity, diabetes (type II), as well as alcoholism can lead to fatty infiltration of the liver (steatosis), steatohepatitis, and cirrhosis.

4. Viral: Viral hepatitis, mainly caused by the hepatitis B and hepatitis C viruses, is currently the most important etiologic factor leading to liver fibrosis and cirrhosis in North America.

Currently Used Terminology

Since 1995, a modified nomenclature has categorized hepatic nodules into two groups: regenerative lesions and dysplastic or neoplastic lesions (7).

Regenerative nodules result from localized proliferation of hepatocytes and their supporting stroma. Regenerative lesions include monoacinar regenerative nodules, multiacinar regenerative nodules, cirrhotic nodules, segmental or lobar hyperplasia, and FNH.

A monoacinar or multiacinar regenerative nodule is a well-defined region of parenchyma that has enlarged in response to necrosis, altered circulation, or other stimuli. It may contain one (monoacinar) or multiple (multiacinar) portal tracts. The diameter of monoacinar nodules is usually 0.1–10 mm, and that of multiacinar nodules should be at least 2 mm. Large multiacinar nodules are usually 5–15 mm in diameter. Cirrhotic nodules are regenerative nodules that are largely or completely surrounded by fibrous septa. Cirrhotic nodules can be mono- or multiacinar. Macronodular cirrhosis contains nodules larger than 3 mm in diameter (7).

Dysplastic or neoplastic lesions are composed of hepatocytes that show histologic characteristics of abnormal growth caused by a presumed or proved genetic alteration. Dysplastic or neoplastic

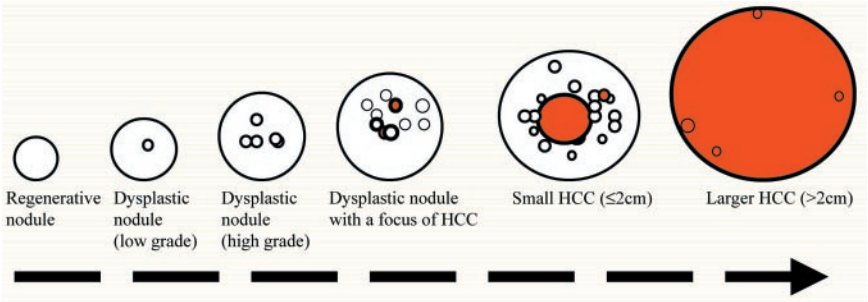

Figure 1. Stepwise pathway of carcinogenesis for HCC in cirrhosis. One or more regenerative nodules may show signs of atypia (○) and change into dysplastic nodules. Atypia indicates a number of changes in the shape and size of the nuclei and the cytoplasm of the hepatocytes. These changes often result in an increased number of cells (increased cellularity), which may be present in groups of small cells (small cell dysplasia) or large cells (large cell dysplasia). Atypia within dysplastic nodules can progress further and give rise to small and large HCCs. In addition to the cellular changes, the hepatic parenchymal structure will often be distorted in HCC. (Adapted and reprinted, with permission, from reference 1.)

nodules include hepatocellular adenoma, dysplastic foci, dysplastic nodules, and HCC.

A dysplastic focus is defined as a cluster of hepatocytes less than 1 mm in diameter with dysplasia but without definite histologic criteria for malignancy. Dysplasia indicates the presence of nuclear and cytoplasmic changes, such as minimal to severe nuclear atypia and an increased amount of cytoplasmic fat or glycogen, within the cluster of cells that compose the focus. Dysplastic foci are common in cirrhosis and uncommon in noncirrhotic livers. The dysplasia can be of the small or large cell type (7).

A dysplastic nodule is a nodular region of hepatocytes at least 1 mm in diameter with dysplasia but without definite histologic criteria for malignancy. These nodules are usually found in cirrhotic livers. Dysplastic nodules can be low grade or high grade (7). Nodules with low-grade dysplasia may show an altered liver parenchymal structure as well as an increased number of cells with an increased nuclei-to-cytoplasm ratio. Nodules with high-grade dysplasia show increased thickness of the layers of hepatocytes, which contain nuclei that are variable in size and shape.

HCC is a malignant neoplasm composed of cells with hepatocellular differentiation. A small HCC is defined as less than or equal to 2 cm in diameter. The criteria used to distinguish HCC from high-grade dysplastic nodules are not clearly defined. Criteria in favor of malignancy include (*a*) prominent nuclear atypia; (*b*) a high nuclear-cytoplasmic ratio with nuclear density twice as great as normal; (*c*) plates three or more cells thick, numerous unaccompanied arteries; (*d*) mitoses in moderate numbers; and (*e*) invasion of the stroma or portal tracts. Most small HCCs cannot be distinguished histologically from dysplastic nodules with certainty. In addition, foci of carcinoma can be found in otherwise benign dysplastic nodules. These and other findings support the theory of stepwise carcinogenesis of HCC (7).

Pathways of Carcinogenesis

A stepwise carcinogenesis for HCC has been proposed on the basis of gradually increasing size and cellular density among the following lesions: regenerative nodules, adenomatous hyperplasia, atypical adenomatous hyperplasia, early HCC, and early advanced HCC (8,9). According to the currently used terminology, the stepwise sequence of events (regenerative nodule to adenomatous hyperplasia to atypical adenomatous hyperplasia to early HCC to early advanced HCC) can be translated as follows: regenerative nodule, low-grade dysplastic nodule, high-grade dysplastic nodule, small HCC, and large HCC (Fig 1). Several authors have proposed a de novo pathway for HCC in cirrhotic as well as noncirrhotic livers (1,8,9). According to the de novo pathway, a single cell or a group of hepatocytes may give rise to a focus of small HCC that will grow into a large HCC (1).

At some point during the whole process of carcinogenesis for HCC (most likely when regenerative nodules become dysplastic nodules), formation of new tumor vessels (tumor angiogenesis, neovascularity) takes place (1). The appearance

of new tumor vessels is important in the transformation of regenerative nodules into dysplastic nodules and small HCCs. Neoangiogenesis is also important for sustained growth of HCC. In addition, neovascularity within HCC can be used for early detection and characterization of these lesions with imaging.

Histopathologic Features

The histologic grade of tumor differentiation is assigned by using the Edmondson grading system (10,11). At histologic analysis, it may be difficult to differentiate among hepatocellular nodules (Fig 2). Depending on tumor differentiation, one hepatocellular lesion may contain one or more clonelike cell populations, and these cell populations can be graded from I to IV. Grade I consists of cells that are similar in size to normal hepatocytes and arranged in relatively thin trabeculae. Acini containing bile are rare. Grade II consists of cells that are larger than normal hepatocytes with more hyperchromatic nuclei, which occupy a higher proportion of cells. The trabeculae are thicker, and acini with bile are common. Grade III consists of hepatocytes with larger nuclei, occupying more than 50% of the cytoplasm. The trabeculae are still dominant, but solid areas and isolated cells may also be present. In addition, giant and bizarre cells are common. Bile is rarely present. Grade IV consists of cells with nuclei occupying most of the cytoplasm, and the cytoplasm may not be eosinophilic. Mostly solid areas are found. Bile is rarely found. Intravascular and intrasinusoidal growth is commonly present. With this grading system, grade I cell populations may be difficult to distinguish from hepatocellular adenomas, and grade IV cell populations may be difficult to distinguish from tumors of nonhepatocellular origin (10).

The classic macroscopic classification of HCC by Eggle has been used since 1901. According to this classification, Edmondson and Steiner (10) categorized 70 HCCs in their series as nodular (81%), massive (23%), and diffuse (3%). This classification is mainly based on autopsy cases of HCC. Compared with the massive lesions, the nodular tumors are smaller and more distinct with sharper margins to the liver (10). The massive lesions are either composed of confluent smaller tumors or consist of predominantly one large lesion that often occupies almost the entire liver. The diffuse lesions consist of multiple infiltrating lesions that occupy a large part of the liver (10).

MR Imaging Features

Focal Nodular Hyperplasia

FNH is a benign liver tumor that occurs predominantly in women during their reproductive years, but cases have been reported in men and children (12–14). FNH is lobulated and well circumscribed, although unencapsulated (13). The pathognomonic macroscopic feature is a central stellate scar with radiating septa, thereby dividing the lesion into numerous nodules of normal hepatocytes that are abnormally arranged (13,15). The central scar contains thick-walled vessels with sources from the hepatic artery, which provides excellent arterial blood supply to the lesion (16). The most characteristic microscopic features of FNH are the fibrous septa and the areas of hepatocellular proliferation (15). The nodules within FNH lack normal central veins and portal tracts. The bile ducts seen within the central scar do not connect to the biliary tree (15). According to the International Working Party (7), FNH is considered a regenerative benign nodule. FNH is often an incidental finding at imaging studies and needs to be differentiated from other focal liver lesions such as HCC, hepatocellular adenoma, and hypervascular metastases (1,17). Most cases of FNH do not need treatment (17).

At MR imaging, FNH is slightly hypointense on T1-weighted images and slightly hyperintense on T2-weighted images (6). FNH may also be nearly isointense on both T1- and T2-weighted images (6). Unlike liver cell adenomas, FNH rarely has higher signal intensity than the liver on T1-weighted images (1,6). The central scar usually has high signal intensity on T2-weighted images (14). FNH shows very intense homogeneous enhancement during the arterial phase of a

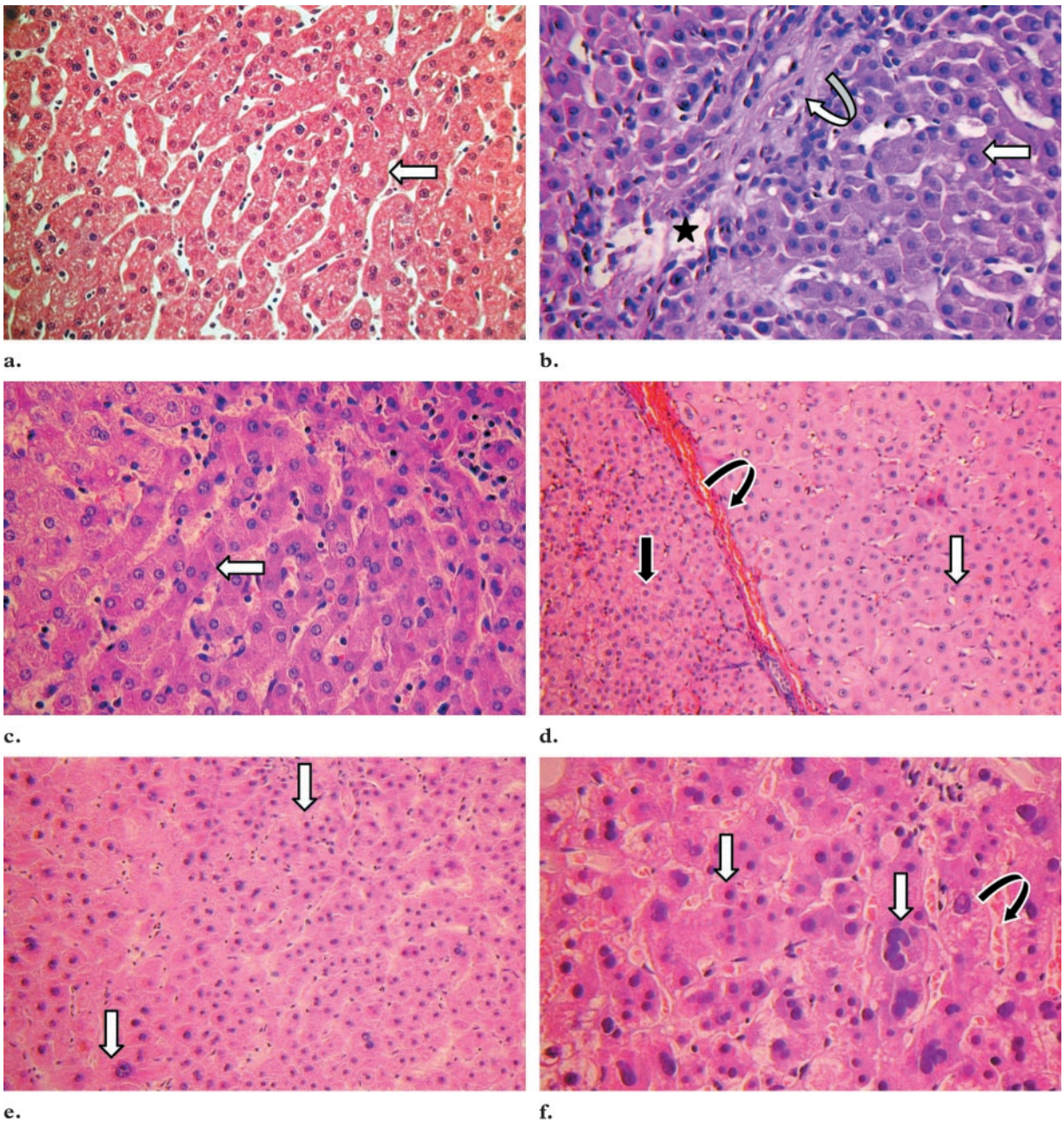

Figure 2. Histologic features of normal liver tissue, FNH, hepatocellular adenoma, regenerative nodules with low-grade dysplasia, regenerative nodules with high-grade dysplasia, and HCC. **(a)** Photomicrograph of normal hepatic parenchyma (original magnification, ×400; hematoxylin-eosin [H-E] stain) shows the hepatocytes arranged in single-cell layers and separated by sinusoids (arrow). Note that the nuclei and the cytoplasm have a similar appearance throughout the specimen. **(b)** Photomicrograph of a biopsy specimen from a hepatic tumor (original magnification, ×400; H-E stain) shows normally arranged hepatocytes (straight arrow) and a fibrous septum (curved arrow) containing biliary structures (★). These findings are compatible with the diagnosis of FNH. **(c)** Photomicrograph of hepatocellular adenoma (original magnification, ×400; H-E stain) shows more or less normal hepatocytes arranged in one- or two-cell layers (arrow). The tumor did not contain any fibrous septa or biliary structures. This combination of findings is typical of hepatocellular adenoma at histopathologic analysis. **(d)** Photomicrograph of two neighboring regenerative nodules (original magnification, ×200; H-E stain) that are separated by a septum (curved arrow) shows an altered hepatic parenchymal structure, as well as an increased number of cells with small cell dysplasia and nuclear crowding in one nodule (black straight arrow) and large cell dysplasia consisting of larger hepatocytes with larger nuclei in the other nodule (white arrow). The findings are compatible with low-grade dysplasia. **(e)** Photomicrograph of high-grade dysplasia (original magnification, ×200; H-E stain) shows increased thickness of the layers of hepatocytes, which contain nuclei that are variable in size and shape (arrows). **(f)** Photomicrograph of HCC (original magnification, ×400; H-E stain) shows large polymorphous hepatocytes arranged in thick layers (straight arrows). Note the large number of vascular structures containing erythrocytes (curved arrow), which indicate tumor angiogenesis.

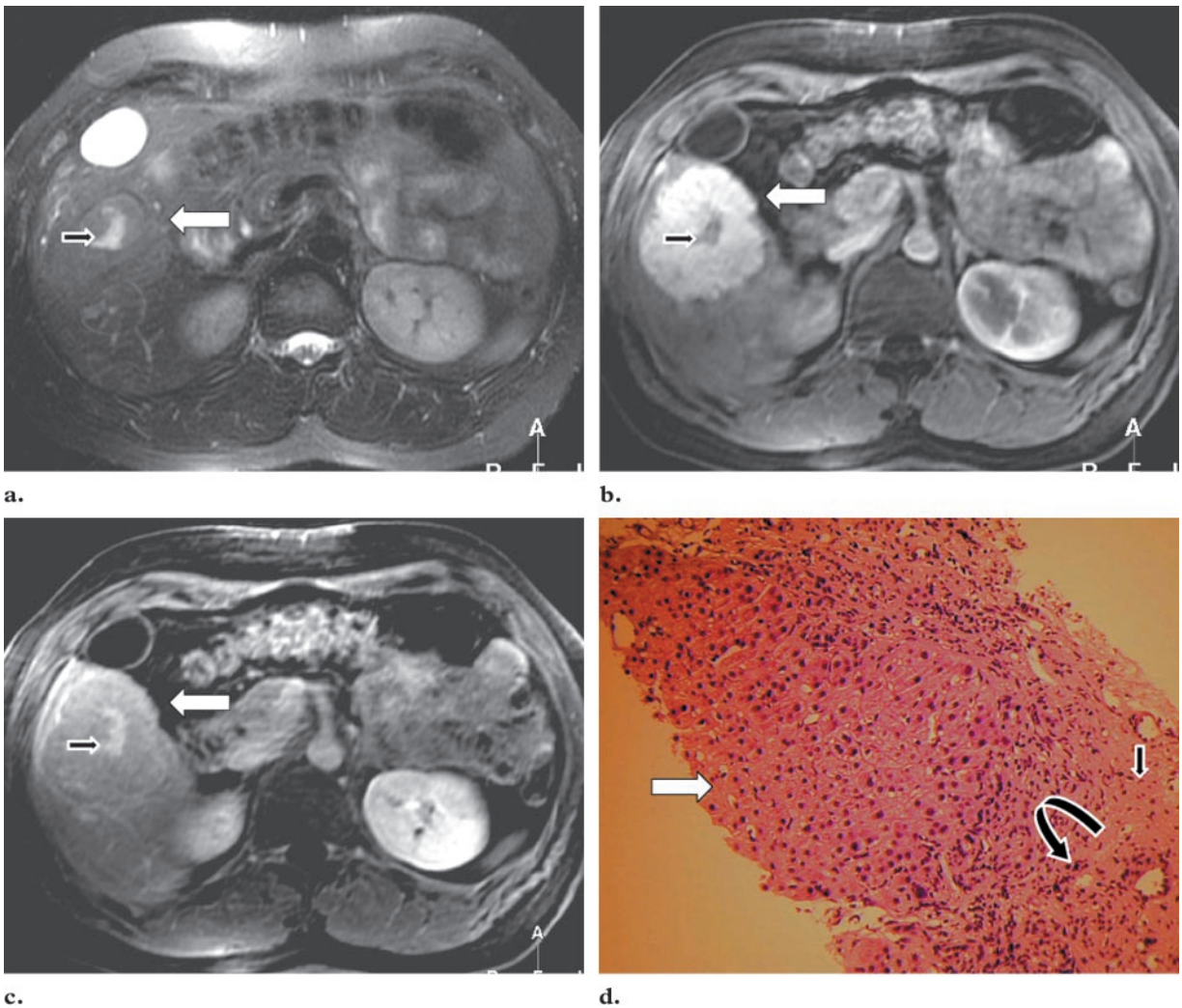

Figure 3. FNH. **(a)** Axial T2-weighted fat-saturated fast spin-echo MR image shows a lesion (white arrow) that is predominantly isointense relative to normal hepatic tissue with a bright central scar (black arrow). **(b)** Axial arterial phase dynamic contrast-enhanced three-dimensional gradient-echo MR image shows that the lesion (white arrow) has intense homogeneous enhancement without enhancement of the central scar (black arrow). **(c)** Axial delayed contrast-enhanced gradient-echo MR image shows that the lesion (white arrow) is isointense relative to normal hepatic tissue with enhancement of the central scar (black arrow). **(d)** Photomicrograph of a biopsy specimen (original magnification, ×200; H-E stain) shows normally arranged hepatocytes (white arrow) and a fibrous septum (black straight arrow) containing biliary structures (curved arrow). This combination of findings is consistent with FNH.

dynamic contrast-enhanced sequence (1,6,14). The central scar and the radiating septa show enhancement on delayed images (Fig 3) (14).

Hepatocellular Adenoma

Liver adenomas typically occur in young women using oral contraceptives (6). These tumors were rarely reported in the medical literature before the introduction of oral contraceptives in the early 1960s. An association with other conditions or hepatocellular stimulating agents, such as familial diabetes mellitus, galactosemia, glycogen storage disease type 1, and anabolic steroids, has been reported (6). Liver cell adenomas are composed of sheets of cells that may resemble normal hepatocytes (7,17,18). Unlike FNH, liver cell adeno-

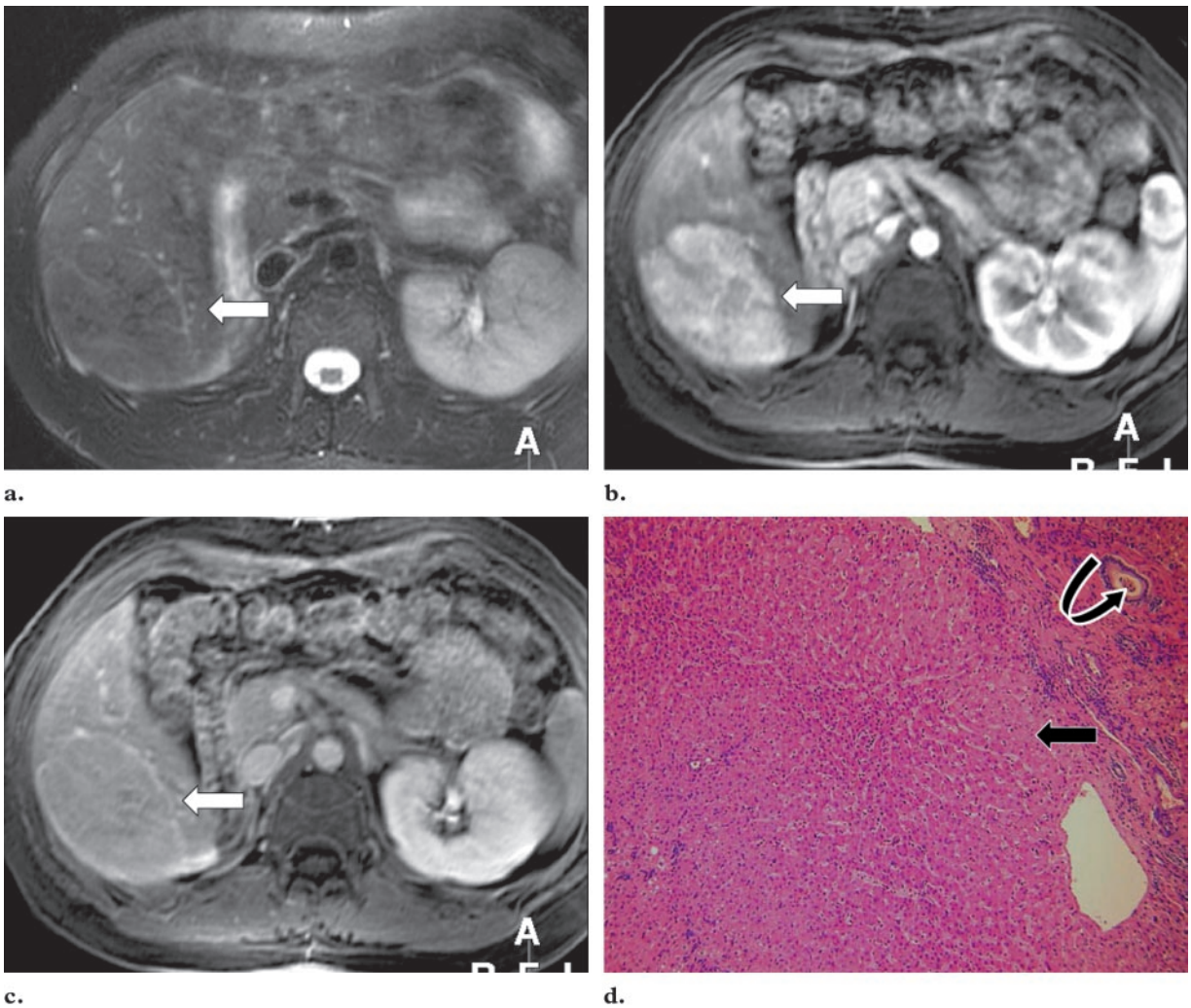

Figure 4. Hepatocellular adenoma. **(a)** Axial T2-weighted fat-saturated fast spin-echo MR image shows a lesion (arrow) that is isointense relative to normal hepatic tissue. No central scar is present. **(b)** Axial arterial phase dynamic contrast-enhanced three-dimensional gradient-echo MR image shows that the lesion (arrow) has intense homogeneous enhancement. **(c)** Axial delayed contrast-enhanced gradient-echo MR image shows that the lesion (arrow) is isointense relative to normal hepatic tissue with enhancement of a pseudocapsule. **(d)** Photomicrograph (original magnification, ×200; H-E stain) shows that the lesion consists of almost normally arranged hepatocytes (straight arrow); however, there are no portal vein tracts within the tumor. Normal portal vein tracts (curved arrow) are present within the compressed hepatic parenchyma surrounding the tumor.

mas lack a central scar and radiating septa. Necrosis and hemorrhage are frequent causes of pain (6). In addition, according to the currently used terminology, hepatocellular adenomas are classified as premalignant nodules (7). Owing to their potential for hemorrhage and malignant degeneration, hepatocellular adenomas are preferably treated surgically (17).

At MR imaging, liver adenomas typically do not differ much in signal intensity from the surrounding liver parenchyma on T1- and T2-weighted images. The lesions are mildly hypointense to moderately hyperintense on T1-weighted images and mildly hyperintense on T2-weighted images (6). They show a blush of homogeneous enhancement in the arterial phase and become nearly isointense in later phases of dynamic gadolinium-enhanced imaging (Fig 4).

Figure 5. Regenerative nodules in a cirrhotic liver with MR imaging–histopathologic correlation. **(a)** Axial T2-weighted fat-saturated fast spin-echo MR image shows an irregular hepatic contour and multiple small hypointense nodules. The liver is surrounded by hyperintense ascites. **(b)** Axial T1-weighted spoiled gradient-echo MR image obtained during the arterial phase shows intense enhancement of the aorta (white arrow). There are no enhancing lesions within the liver. Black arrow = ghost artifact. **(c)** Axial delayed contrast-enhanced T1-weighted gradient-echo MR image obtained with fat saturation shows enhancement of the portal vein (white arrow). Within the liver, multiple small regenerative nodules are visible within enhancing septa. Black arrow = ghost artifact. **(d)** Photograph of a section of the explanted liver shows that the liver is shrunken with an irregular surface (arrows), which is consistent with multiple regenerative nodules. **(e)** Photomicrograph (original magnification, ×100; H-E stain) shows a regenerative nodule surrounded by septa (curved arrow), which contain a number of portal vein tracts (straight arrows).

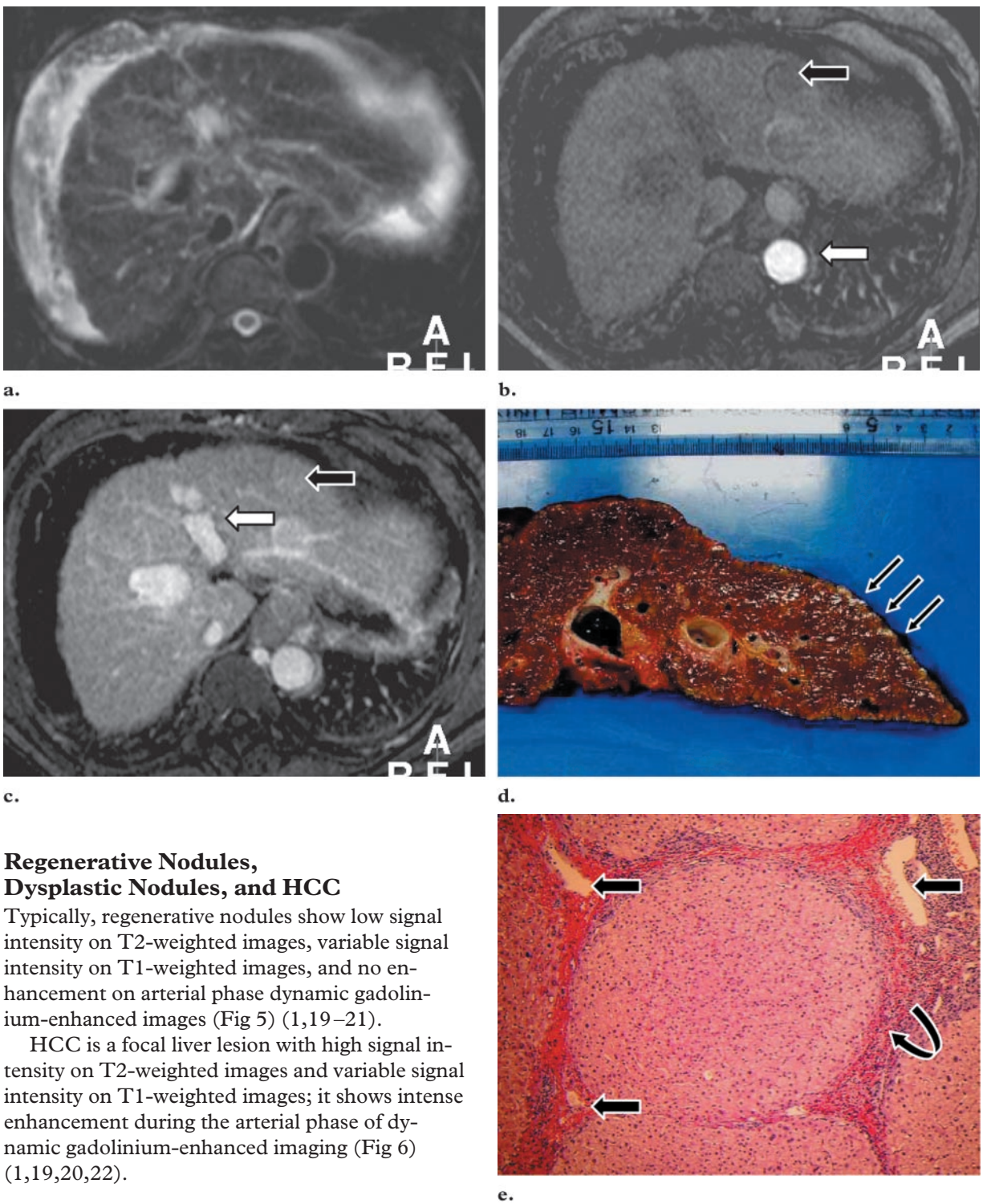

a. b. c. d. e.

Regenerative Nodules, Dysplastic Nodules, and HCC

Typically, regenerative nodules show low signal intensity on T2-weighted images, variable signal intensity on T1-weighted images, and no enhancement on arterial phase dynamic gadolinium-enhanced images (Fig 5) (1,19–21).

HCC is a focal liver lesion with high signal intensity on T2-weighted images and variable signal intensity on T1-weighted images; it shows intense enhancement during the arterial phase of dynamic gadolinium-enhanced imaging (Fig 6) (1,19,20,22).

Figure 6. HCC within a dysplastic nodule with MR imaging–histologic correlation. **(a)** Axial T2-weighted fat-saturated fast spin-echo MR image shows multiple low-signal-intensity regenerative nodules and a larger brighter lesion (arrow). **(b)** Axial in-phase T1-weighted gradient-echo MR image shows multiple bright nodules with variable sizes. The larger lesion is visible, at least in part, as a bright nodule (arrow). **(c)** Axial arterial phase dynamic contrast-enhanced T1-weighted gradient-echo MR image shows that part of the larger lesion enhances (white arrow). Black arrow = ghost artifact. **(d)** Photomicrograph of a specimen obtained with ultrasonographically guided biopsy from the larger lesion (original magnification, ×400; H-E stain) shows hepatocytes with high-grade dysplasia (arrow) next to moderately differentiated HCC with some fatty infiltration (★). HCC consists of polymorphous hepatocytelike cells with loss of the normal parenchymal architecture of the liver.

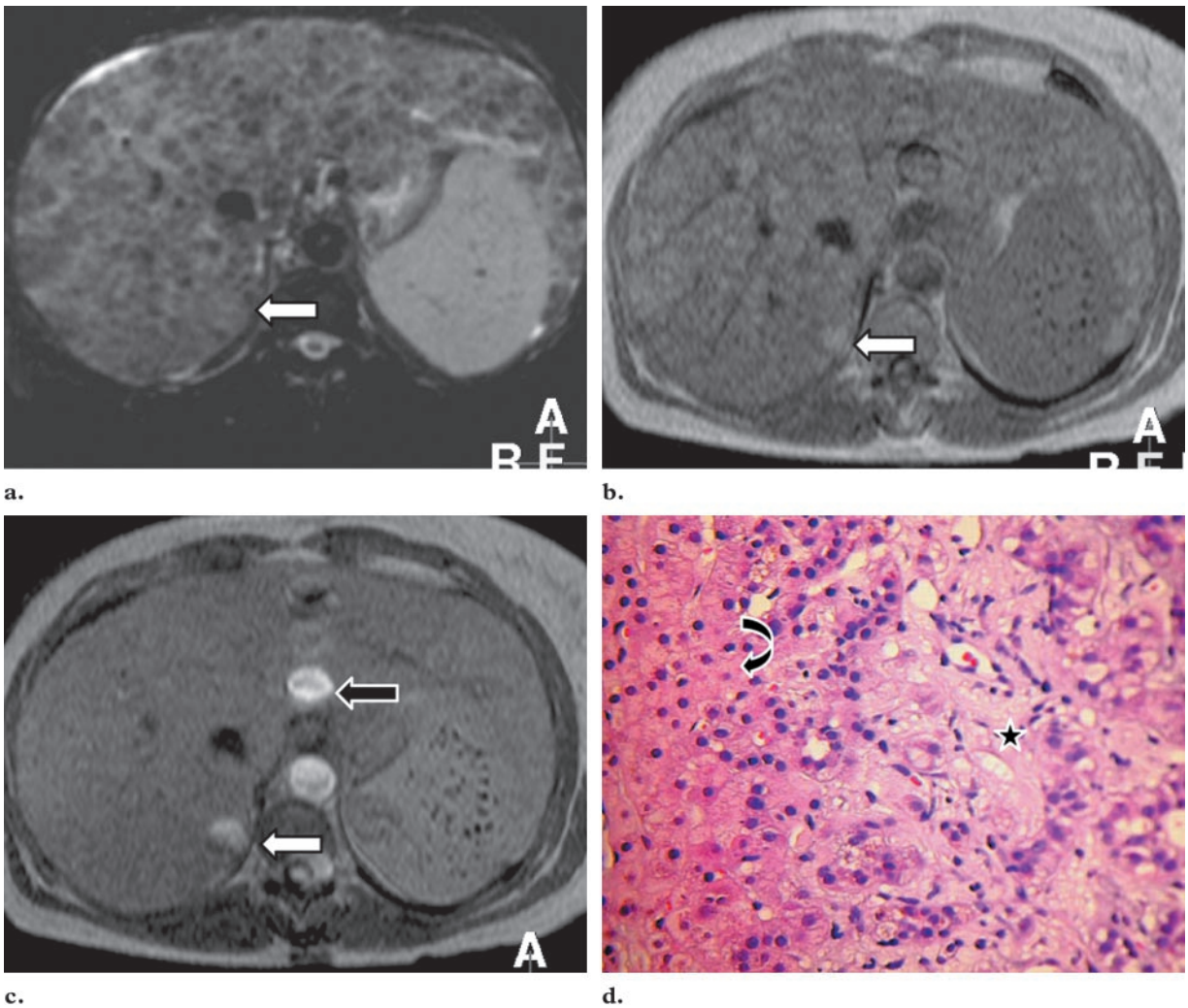

The signal intensity and enhancement characteristics of dysplastic nodules are not yet well established. Owing to a gradual stepwise transition from a regenerative nodule to a low-grade dysplastic nodule, a high-grade dysplastic nodule, and eventually to a small HCC and a large HCC, the hepatocytes within hepatic nodules undergo numerous changes that might not be reflected in their signal intensity or vascularity. Thus, current MR imaging sequences might not allow differentiation of regenerative nodules from dysplastic nodules with certainty. Some MR imaging features of high-grade dysplastic nodules and small HCC have been described (1,2,19–21). A majority of high-grade dysplastic lesions (formerly known as *adenomatous hyperplasia*) and well-differentiated small HCCs (Edmondson grade I or II) have high signal intensity on T1-weighted images (Fig 6) (19–21).

Small HCC

Recent MR imaging techniques allow thinner sections with higher matrices in combination with high intrinsic soft-tissue contrast. In addition, faster imaging sequences allow imaging with sufficiently higher temporal resolution to capture the distinct arterial and other phases of enhancement of liver lesions during gadolinium-enhanced imaging (1).

Figure 7. Small HCC with MR imaging–pathologic correlation. **(a)** Axial T2-weighted single-shot fast spin-echo MR image shows a small isointense nodule (arrow). **(b)** Axial arterial phase dynamic contrast-enhanced two-dimensional gradient-echo MR image shows intense enhancement of the lesion (arrow). **(c)** Axial portal phase dynamic contrast-enhanced two-dimensional gradient-echo MR image shows somewhat less intense enhancement of the lesion (arrow). **(d)** Photograph of a section of the explanted liver, obtained 3 months after the MR imaging examination, shows a slight increase in the size of the HCC (thick straight arrow). In the center of the HCC, two linear necrotic areas are present (curved arrow), which were induced by laser treatment 2–3 months before surgery. Note the multiple small regenerative nodules (thin straight arrow).

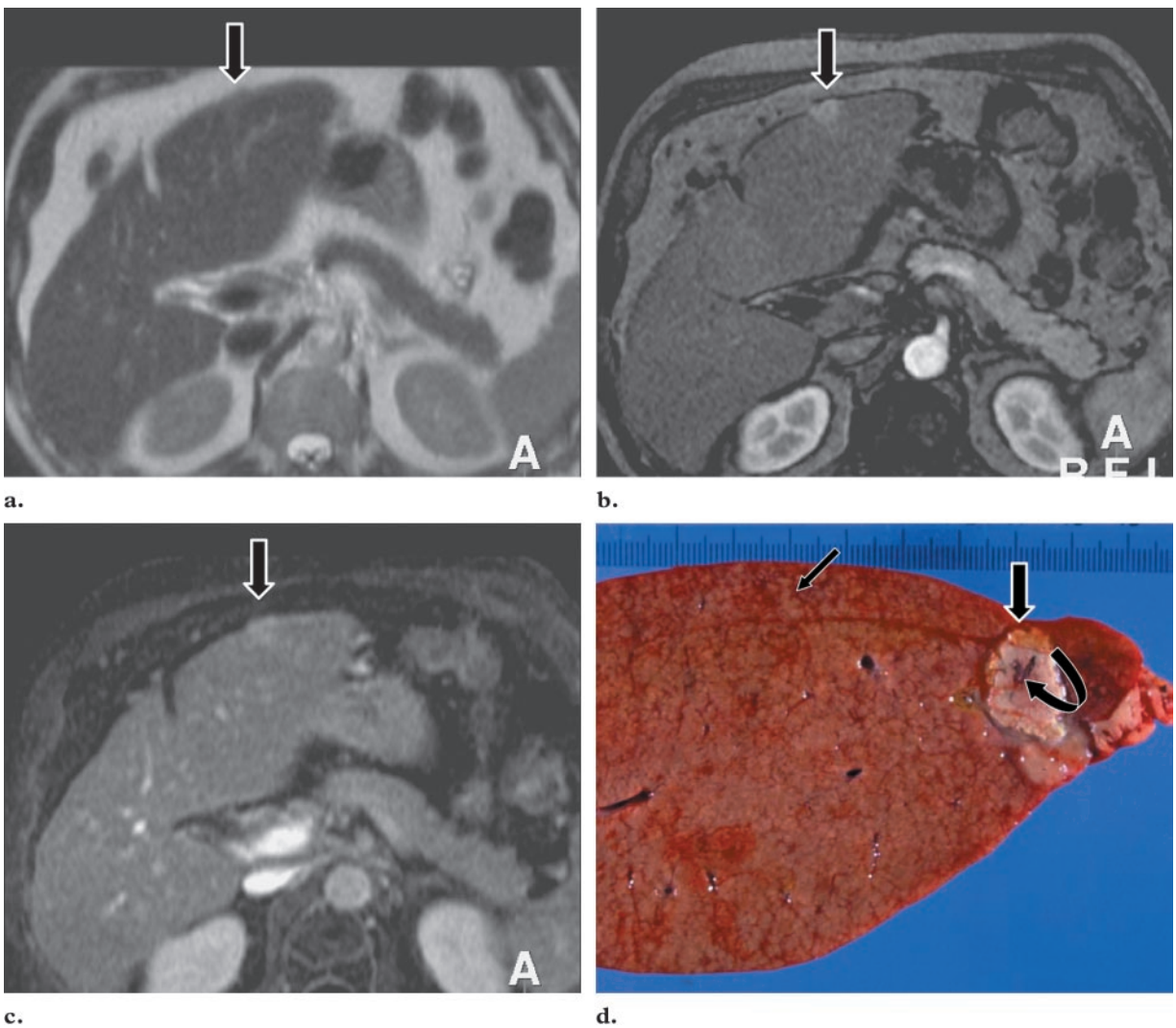

This facilitates detection of smaller HCCs (2). The definition of small tumors has changed, from a solitary lesion less than 4.5 cm in diameter to a tumor less than or equal to 2 cm in diameter (2).

High-grade dysplastic nodules and small HCC may have a nodule-within-a-nodule appearance on MR images, especially if a focus of HCC originates within a siderotic regenerative nodule (23). On T2-weighted images, this appearance may consist of low signal intensity of a large nodule, with one or more internal foci of higher signal intensity. On T1-weighted gradient-echo images, such lesions typically show markedly low signal intensity of a large nodule, with internal foci that are isointense to the liver. At MR imaging, the recognition of HCC while still small is important because the tumor is aggressive and has a fast doubling time (24). Small HCC may also appear as small areas of slightly higher signal intensity than the surrounding liver on T2-weighted images. On T1-weighted images, such areas may be isointense, hypointense, or hyperintense to the liver. On arterial phase dynamic gadolinium-enhanced images, most small HCCs show intense enhancement (Fig 7). The MR imaging appearance of such areas suggests a replacing, instead of an expanding, type of growth (11).

Large HCC

Large HCC may have a number of characteristic features, such as a mosaic pattern, a tumor capsule, extracapsular extension with formation of

Figure 8. Large HCC with a mosaic pattern, a tumor capsule, and fatty infiltration. **(a)** Axial T2-weighted single-shot fast spin-echo MR image shows a lesion with areas of low and high signal intensity (arrow). **(b, c)** In-phase **(b)** and opposed-phase **(c)** axial T1-weighted gradient-echo MR images show a marked decrease in signal intensity in part of the lesion (arrow), which is due to fatty infiltration. **(d)** Axial fat-saturated delayed contrast-enhanced MR image shows enhancement of a tumor capsule (arrow). **(e)** Photomicrograph of a biopsy specimen (original magnification, ×40; H-E stain) shows the HCC surrounded by the fibrous capsule (straight arrow). Owing to fatty infiltration, part of the tumor (curved arrow) appears more whitish than the other part of the lesion (★). These findings reflect the mosaic appearance of the encapsulated lesion at MR imaging.

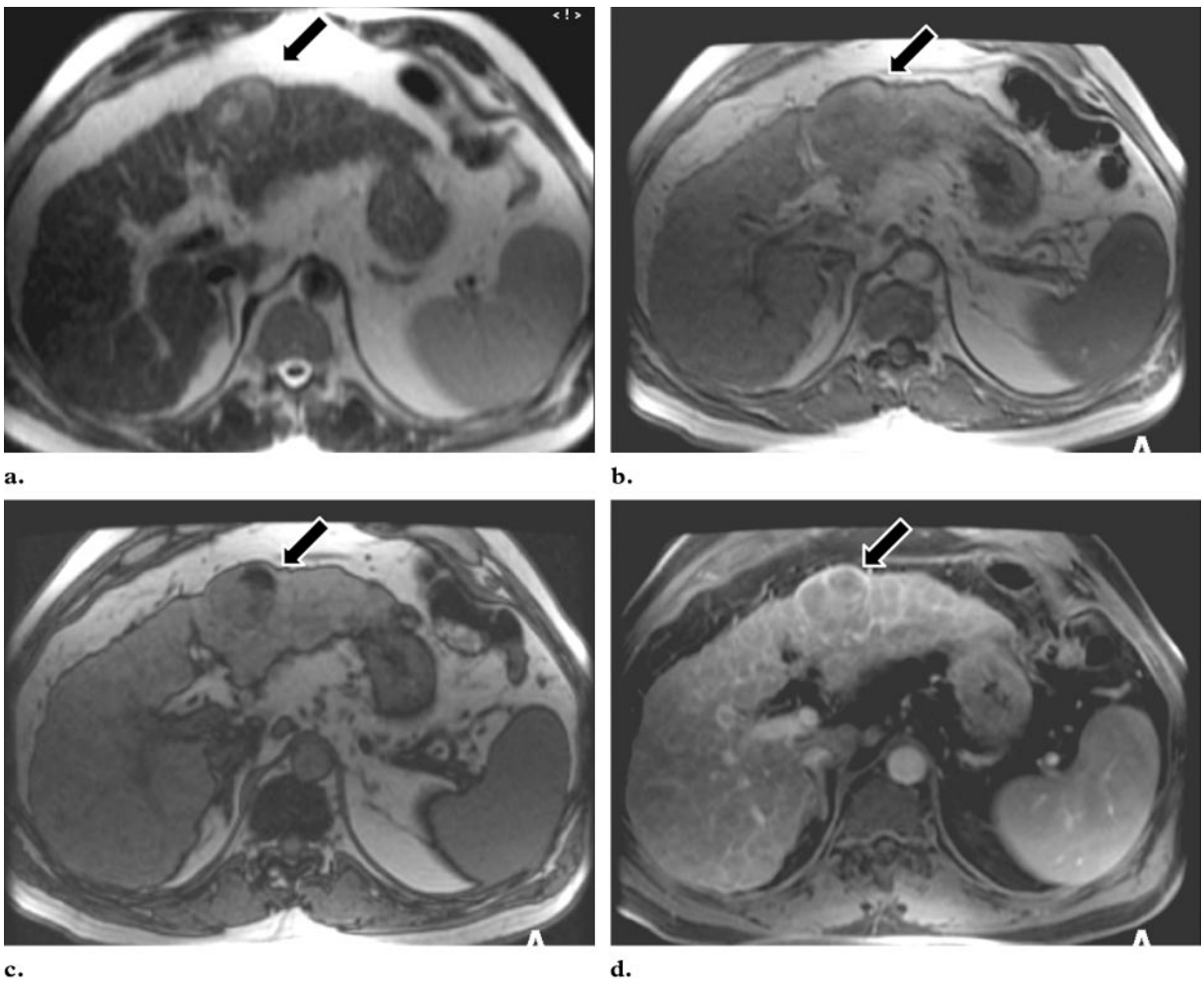

a. b. c. d.

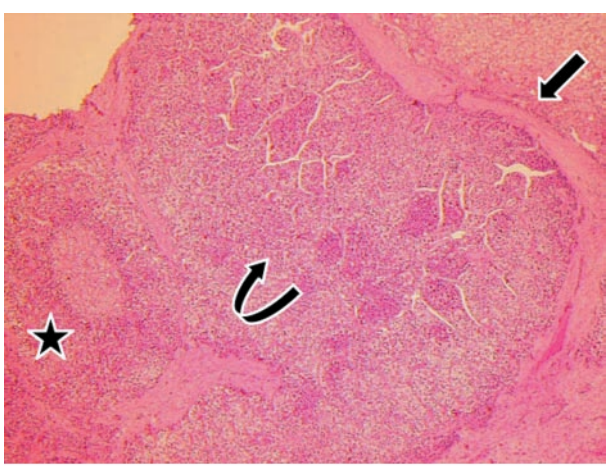

e.

satellite nodules, vascular invasion, and extrahepatic dissemination, including lymph node and distant metastases (1).

The mosaic pattern is a configuration of confluent small nodules separated by thin septa and necrotic areas within the tumor. This appearance most likely reflects the histopathologic features as well as the characteristic growth pattern of HCC. In one study, 88% of lesions with a mosaic pattern were larger than 2 cm in diameter (25). The mosaic pattern is more often depicted on T2-weighted images than on T1-weighted images (25). On T1- and T2-weighted images, the mosaic pattern appears as areas of variable signal intensities, whereas on gadolinium-enhanced images, the lesions enhance in a heterogeneous fashion during the arterial and later phases (25). The degree of histologic differentiation, the presence of copper protein, and fatty infiltration may all be responsible for the mosaic pattern (Fig 8).

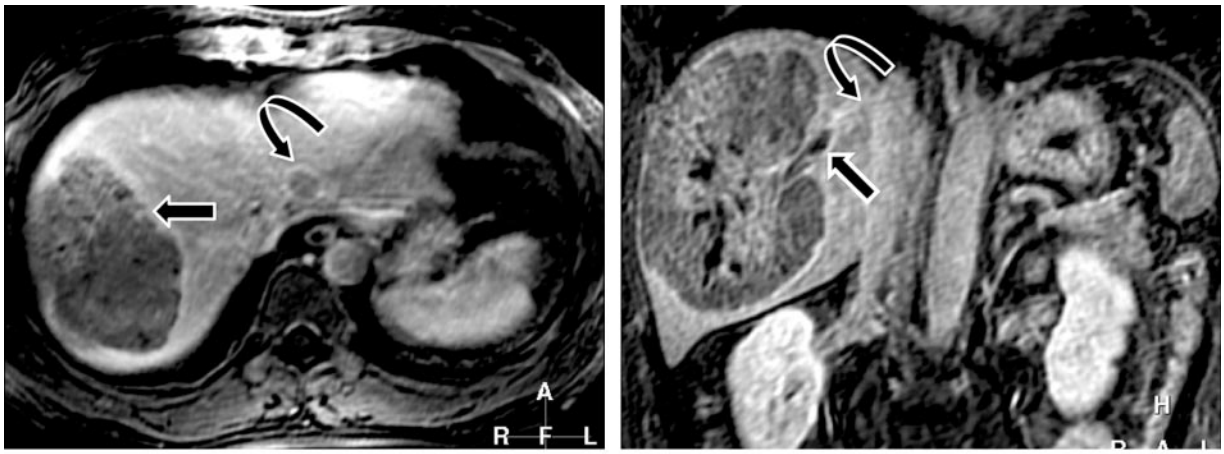

a. b.

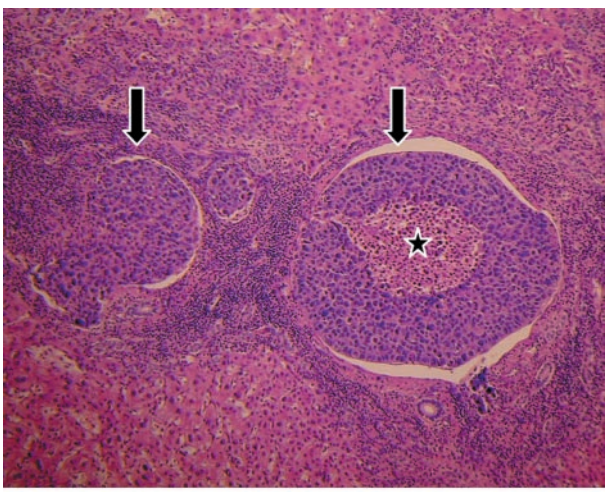

c.

Figure 9. Large HCC with a satellite nodule and vascular invasion. **(a)** Axial portal phase dynamic gadolinium-enhanced three-dimensional fat-saturated gradient-echo MR image shows heterogeneous enhancement of a large HCC (straight arrow) as well as a satellite lesion (curved arrow). **(b)** Coronal contrast-enhanced gradient-echo MR image shows that one of the hepatic veins lacks homogeneous enhancement within the proximal part of the vessel due to a tumor thrombus (straight arrow). Note that the distal part of the hepatic vein as well as the inferior vena cava enhance normally (curved arrow). **(c)** Photomicrograph (original magnification, ×100; H-E stain) shows vascular invasion (arrows). Note the central necrosis within one of the tumor thrombi (★).

A tumor capsule, a characteristic sign of large HCC, is present in 60%–82% of cases (25) (Fig 8). In one study, 56 of 72 HCCs showed a capsule at histologic analysis, and 75% of the lesions with a capsule were larger than 2 cm in diameter (25). The tumor capsule becomes thicker with increasing tumor size (25). At histologic analysis, capsules are composed of two layers, an inner fibrous layer and an outer layer containing compressed vessels and bile ducts (25). The tumor capsule is hypointense on both T1- and T2-weighted images in most cases, although capsules with a thickness of more than 4 mm can have an outer hyperintense layer on T2-weighted images. Extracapsular extension of the tumor, with partial projections or formation of satellite nodules in the immediate vicinity, is present in 43%–77% of HCCs (1,26) (Fig 9).

Vascular invasion occurs frequently in HCC and can affect both the portal vein as well as the hepatic veins (1). In a recent study of 322 patients undergoing curative resection of HCC, 15.5% had macroscopic venous invasion and 59.0% had microscopic venous invasion at histopathologic analysis (27). In a meta-analysis of seven studies of 1,497 patients, portal vein invasion was found in 24% of cases of HCC (28). At MR imaging, vascular invasion can be seen as lack of a signal void on multisection T1-weighted gradient-echo and flow-compensated T2-weighted fast spin-echo images (1). On gadolinium-enhanced images, the tumor thrombus typically shows enhancement on images acquired during the arterial phase and a filling defect on images acquired during later phases (Fig 9).

HCC in a Noncirrhotic Liver

In patients without cirrhosis or other underlying liver disease, HCC is usually diagnosed at a very late stage (29). In one study of HCC in the noncirrhotic liver, the medium tumor diameter was 8.8 cm (30). In a recent study of 36 patients with HCC, including 11 with and 25 without cirrhosis, the MR imaging appearance was compared (31). The lesions in noncirrhotic livers were significantly larger, were more often solitary, and more frequently contained a central scar (Fig 10) (31).

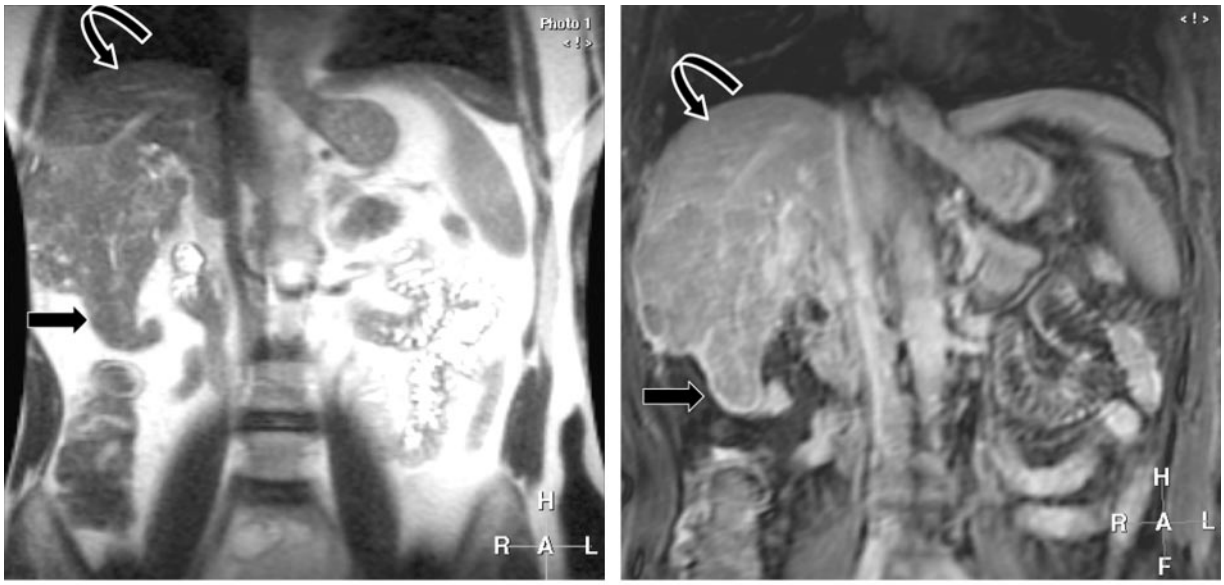

a. b.

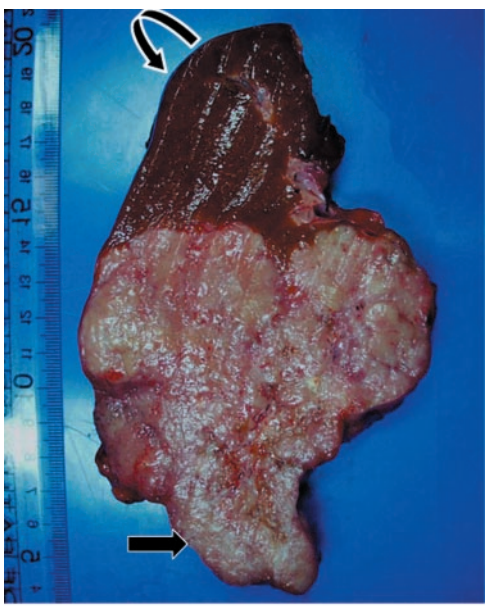

c.

Figure 10. Large HCC in a noncirrhotic liver. **(a)** Coronal single-shot fast spin-echo MR image shows a large tumor (straight arrow) with predominantly high signal intensity compared with that of surrounding hepatic tissue (curved arrow). **(b)** Coronal delayed contrast-enhanced three-dimensional fat-saturated gradient-echo MR image shows heterogeneous enhancement of the tumor (straight arrow) and homogeneous enhancement of surrounding hepatic tissue (curved arrow). **(c)** Photograph of a section of the resected tumor (straight arrow) and part of the normal noncirrhotic liver (curved arrow) shows excellent correlation with the MR imaging findings.

Fibrolamellar carcinoma is a malignant hepatocellular tumor with distinct clinical and pathologic differences from conventional HCC (32). Therefore, fibrolamellar carcinoma should be considered a separate entity. Cirrhosis, hepatitis, α-fetoprotein, or other typical risk factors for HCC are usually absent (33). At histologic analysis, the lesions consist of large eosinophilic, polygonal neoplastic cells arranged in sheets, cords, or trabeculae separated by parallel sheets of fibrous tissue (ie, lamellae) (33). Vascular invasion occurs in less than 5% of cases. Regional adenopathy may be present in 50%–70% of patients, and distant metastases are uncommon (20%) (33). At MR imaging, fibrolamellar carcinomas are typically hypointense on T1-weighted images and hyperintense on T2-weighted images (33).

Discussion and Conclusions

Cirrhotic and noncirrhotic livers may contain a number of benign, premalignant, and malignant hepatocellular nodules. Recently, new terminology for hepatocellular lesions has been introduced. In particular, during the past 2 decades, MR imaging has increasingly been applied for evaluation of liver lesions. In many centers, MR imaging has become the modality of choice for assessment of cirrhotic and noncirrhotic liver lesions.

To familiarize readers with the recent developments, this article provides the relevant clinical background information and describes MR imaging features of hepatic nodules with pathologic correlation. State-of-the-art MR imaging with a number of T1- and T2-weighted and multiphasic dynamic contrast-enhanced sequences facilitates detection and characterization of the majority of hepatic nodules, including regenerative nodules, dysplastic nodules, HCC, hepatocellular adenoma, and FNH. After reading this article, the reader will understand the new classification of hepatocellular nodules, the carcinogenesis of HCC, and the typical MR imaging features of hepatic nodules.

References

1. Hussain SM, Semelka RC, Mitchell DG. MR imaging of hepatocellular carcinoma. Magn Reson Imaging Clin N Am 2002; 10:31–52.
2. Choi BI, Takayasu K, Han MC. Small hepatocellular carcinoma and associated lesions of the liver: pathology, pathogenesis, imaging findings. AJR Am J Roentgenol 1993; 160:1177–1187.
3. Mitchell DG. Liver I: currently available gadolinium chelates. Magn Reson Imaging Clin N Am 1996; 4:37–51.
4. Katyal S, Oliver JH, Peterson MS, et al. Extrahepatic metastases of hepatocellular carcinoma. Radiology 2000; 216:698–703.
5. Schalm SW. The diagnosis of cirrhosis: clinical relevance and methodology. J Hepatol 1997; 27: 1118–1119.
6. Semelka RC, Ascher SM, Reinhold C. MRI of the abdomen and pelvis: a text-atlas. New York, NY: Wiley-Liss, 1997; 73–82.
7. Terminology of nodular hepatocellular lesions. International Working Party. Hepatology 1995; 22:983–993.
8. Sakamoto M, Hirohashi S, Shimosato Y. Early stages of multistep hepatocarcinogenesis: adenomatous hyperplasia and early hepatocellular carcinoma. Hum Pathol 1991; 22:172–178.
9. Okuda K. Hepatocellular carcinoma: recent progress. Hepatology 1992; 15:948–963.
10. Edmondson HA, Steiner PE. Primary carcinoma of the liver: a study of 100 cases among 18,900 necropsies. Cancer 1954; 7:462–503.
11. Kanai T, Hirohashi S, Upton MP, et al. Pathology of small hepatocellular carcinoma: a proposal for a new gross classification. Cancer 1987; 60:810–819.
12. Pain JA, Gimson AE, Williams R, Howard ER. Focal nodular hyperplasia of the liver: results of treatment and options in management. Gut 1991; 32:524–527.
13. Mathieu D, Vilgrain V, Mahfouz AE, et al. Benign liver tumors. Magn Reson Imaging Clin N Am 1997; 5:255–288.
14. Mortele KJ, Praet M, Van Vlierberghe H, Kunnen M, Ros PR. CT and MR imaging findings in focal nodular hyperplasia of the liver: radiologic-pathologic correlation. AJR Am J Roentgenol 2000; 174:705–712.
15. Shirkhoda A, Farah MC, Bernacki E, et al. Hepatic focal nodular hyperplasia: CT and sonographic spectrum. Abdom Imaging 1994; 19:34–38.
16. Nguyen BN, Flejou JF, Terris B, et al. Focal nodular hyperplasia of the liver: a comprehensive pathologic study of 305 lesions and recognition of new histologic forms. Am J Surg Pathol 1999; 23: 1441–1454.
17. Terkivatan T, de Wilt JHW, de Man RA, et al. Indications and outcome of treatment for benign hepatic tumors: a critical appraisal. Arch Surg 2001; 136:1033–1038.
18. Shortell CK, Schwartz SI. Hepatic adenoma and focal nodular hyperplasia. Surg Gynecol Obstet 1991; 173:426–431.
19. Earls JP, Theise ND, Weinreb JC, et al. Dysplastic nodules and hepatocellular carcinoma: thin-section MR imaging of explanted cirrhotic livers with pathologic correlation. Radiology 1996; 201:207–214.
20. Matsui O, Kadoya M, Kameyama T, et al. Adenomatous hyperplastic nodules in the cirrhotic liver: differentiation from hepatocellular carcinoma with MR imaging. Radiology 1989; 173:123–126.
21. Muramatsu Y, Nawano S, Takayasu K, et al. Early hepatocellular carcinoma: MR imaging. Radiology 1991; 181:209–213.
22. Matsui O, Kadoya M, Kameyama T, et al. Benign and malignant nodules in cirrhotic livers: distinction based on blood supply. Radiology 1991; 178: 493–497.
23. Mitchell DG, Rubin R, Siegelman ES, et al. Hepatocellular carcinoma within siderotic regenerative nodules: appearance as a nodule within a nodule on MR images. Radiology 1991; 178:101–103.
24. Sadek AG, Mitchell DG, Siegelman ES, et al. Early hepatocellular carcinoma that develops within macroregenerative nodules: growth rate depicted at serial MR imaging. Radiology 1995; 195:753–756.
25. Kadoya M, Matsui O, Takashima T, et al. Hepatocellular carcinoma: correlation of MR imaging and histopathologic findings. Radiology 1992; 183:819–825.
26. Imaeda T, Kanematsu M, Mochizuki R, et al. Extracapsular invasion of small hepatocellular carcinoma: MR and CT findings. J Comput Assist Tomogr 1994; 18:755–760.
27. Tsai TJ, Chau GY, Lui WY, et al. Clinical significance of microscopic tumor venous invasion in patients with resectable hepatocellular carcinoma. Surgery 2000; 127:603–608.
28. Lee YT, Geer DA. Primary liver cancer: pattern of metastasis. J Surg Oncol 1987; 36:26–31.
29. Williams R, Rizzi P. Treating small hepatocellular carcinomas. N Engl J Med 1996; 334:728–729.
30. Bismuth H, Chiche L, Castaing D. Surgical treatment of hepatocellular carcinoma in non-cirrhotic liver: experience in 68 liver resections. World J Surg 1995; 19:35–41.
31. Winston CB, Schwartz LH, Fong Y, et al. Hepatocellular carcinoma: MR imaging findings in cirrhotic and noncirrhotic livers. Radiology 1999; 210:75–79.
32. Craig JR, Peters RL, Edmondson HA, et al. Fibrolamellar carcinoma of the liver: a tumor of adolescents and young adults with distinctive clinicopathologic features. Cancer 1980; 46:372–379.
33. McLarney JK, Rucker PT, Bender GN, et al. Fibrolamellar carcinoma of the liver: radiologic-pathologic correlation. RadioGraphics 1999; 19: 453–471.